

Capillary rise and condensation in a cone as an illustration of a spinodal

M. S. Pettersen^{a)}

Department of Physics, Washington and Jefferson College, Washington, Pennsylvania 15301

E. Rolley

Laboratoire de Physique Statistique, de l'Ecole Normale Supérieure, UPMC Université Paris 6, Université Paris Diderot, CNRS, 24 rue Lhomond, 75005 Paris, France

J. Treiner

Espace des Sciences Pierre-Gilles de Gennes, Ecole supérieure de physique et de chimie industrielles, 10 rue Vauquelin, 75005 Paris, France

(Received 15 August 2010; accepted 17 May 2011)

Spinodal decomposition can be observed only in systems whose dynamics are slow enough to quench through the metastable region where the phase transition occurs by nucleation. We discuss the capillary rise of a fluid in a cone inserted into a bulk fluid, with the wide end down. The rise displays a first-order phase transition with a spinodal and is easily accessible both theoretically and experimentally. © 2011 American Association of Physics Teachers.

[DOI: 10.1119/1.3599073]

I. INTRODUCTION

Two phases coexisting at a first-order phase transition have equal free energies. If the thermodynamic conditions (such as temperature or pressure) differ slightly from the conditions for coexistence, the two phases remain local minima of the free energy, but one phase will have a slightly higher free energy than the other: this phase is metastable (see Fig. 1). Examples of metastable states, such as a liquid superheated above its equilibrium boiling point, are common. For the transition from the metastable state to the stable state to occur, the system must overcome a free energy barrier that must be overcome by thermal fluctuations (for a superheated liquid, for instance, these will be thermally excited density fluctuations). Typically, the transition occurs by means of the formation of a nucleus of the stable phase. For example, for a superheated liquid, the minimum work needed to form a bubble of radius r has a positive contribution proportional to r^2 , due to the cost of creating the bubble's surface, and a negative contribution proportional to r^3 , due to the energy gained from converting the interior of the bubble to the stable vapor phase. For small r , the surface tension term dominates, and thus the bubble shrinks; the nucleus must be above its critical size before it can grow, as illustrated in Fig. 2. The energy of the critical nucleus is the free energy barrier.¹⁻³

Far from the equilibrium coexistence curve, one of the phases ceases to be a local minimum of the free energy, and is no longer metastable, but becomes unstable. In this case, there is no energy barrier to the phase transition, and the transition takes place due to the growth of fluctuations at some characteristic (usually microscopic) length scale. The locus of points at which the metastable phase passes into instability forms a curve in the thermodynamic plane called the *spinodal*,⁴ as illustrated schematically in Fig. 1(a). (The spinodal is not a thermodynamically sharp transition except in the mean-field limit. When the energy barrier for decay of a metastable state is on the order of $k_B T$, the lifetime of the metastable state is too short for its free energy to be well defined, and the thermodynamic description is not self-consistent.⁵)

If the system is quenched rapidly enough, it is possible to avoid nucleation and go into the unstable region of the phase diagram. Examples include the separation of glassy solutions and metal alloys,⁶ and polymer blends with immiscible components.⁷ When the phase transition involves chemical separation of immiscible components, as in these examples, it is called *spinodal decomposition*, which can be used to produce metals and ceramics with nanoscale porosity, which have important uses such as catalysis and filtration.⁸

In this paper, we discuss a system consisting of a liquid rising in a cone by capillarity. This system provides a concrete illustration of these ideas and is accessible both experimentally and theoretically to undergraduate physics majors.

II. CAPILLARY RISE IN A CONE

In the usual case of capillary rise in a cylindrical tube, the position of the meniscus is determined by minimizing the free energy of the system, which is the sum of the gravitational potential energy and a term due to surface tension.⁹ For capillary rise in a tube of non-uniform cross section, another term arises from the minimization of the free energy. Where the tube narrows, the surface area A and the surface free energy of the meniscus are both reduced, leading to a force proportional to the derivative of the cross section with height $\partial A/\partial z$, which moves the meniscus in the direction of smaller cross section.

To make these ideas concrete, we consider the energy of the system consisting of a cone with a liquid rising in it, as shown in Fig. 3. We define H to be the height of the apex of the cone above a liquid bath, α the half-angle of the cone, ψ the contact angle of the liquid, and h the height of the meniscus with respect to the bath. (The contact angle, the angle at which the free surface of a liquid meets the surface of a solid when they are in contact, depends on the materials involved, and is governed by the Young-Dupré law.¹⁰) It will be convenient to study the energy of the cone with the meniscus at height h , compared to the energy of the cone when it is completely filled, as a function of the distance from the meniscus to the tip of the cone, $\Delta h = H - h$. Lowering the liquid level

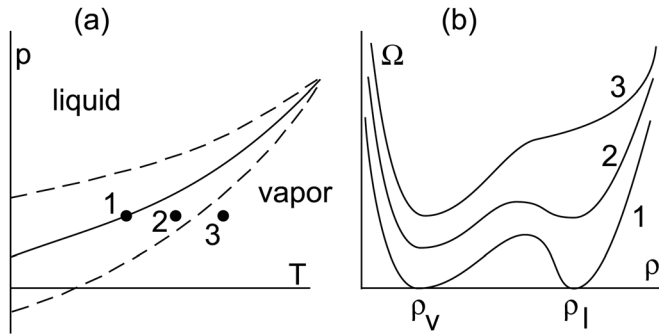


Fig. 1. (a) Phase diagram in the pressure–temperature plane showing the vaporization curve (solid) and the spinodal lines (dashed). At coexistence (point 1), the liquid and vapor are in equilibrium. When the liquid is slightly superheated (point 2) it is metastable; beyond the spinodal (point 3), the liquid is unstable. (b) The Landau free energy Ω as a function of density for values of p and T corresponding to the same three points shown in (a). At coexistence (1), both the equilibrium vapor density ρ_v and liquid density ρ_l represent minima of Ω (and hence are stable states), with equal free energy. If the liquid is slightly superheated (2), both liquid and vapor are local minima of Ω (and hence are stable states), but only the vapor phase is stable (the liquid is metastable). Beyond the spinodal line (3), the free energy has only one minimum, and the liquid state is unstable.

from the tip to the height h will cost the energy of baring the wall surface at the top of the cone, and creating the free surface of the liquid; both terms are proportional to some surface area, and thus are proportional to Δh^2 . In contrast, lowering the liquid gives a gravitational potential energy gain which varies as the volume of the liquid lowered, times the distance it is lowered; thus we expect a potential energy gain that varies roughly as $\Delta h^3(H - \Delta h)$. For sufficiently small Δh , the surface tension term wins, and the meniscus will be drawn up to the apex of the cone, as was noted by Tsori.¹¹ This transition is not restricted to conical geometry, and can arise whenever the cross section of the capillary is not constant. The transition is analogous to the phenomenon of capillary condensation in porous media or wetting transitions in confined geometries, because both transitions originate from competition between potential energy (here, gravity) and interfacial tension energy.¹²

Based on the preceding physical arguments, we expect that the form of the free energy of the system is given by

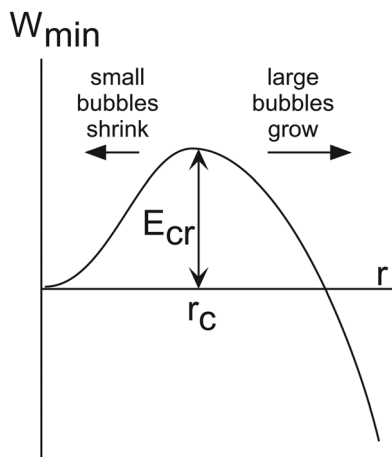


Fig. 2. Minimum work required to form a bubble nucleus as a function of its radius. Below a critical radius r_c the nucleus shrinks instead of growing. E_{cr} is the free energy barrier which must be overcome by thermal fluctuations so that the nucleus can grow.

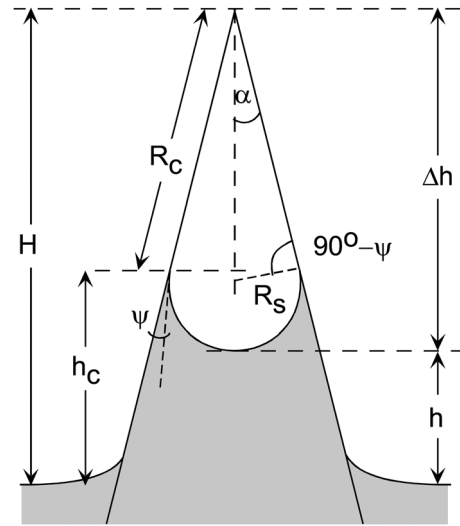


Fig. 3. Capillary rise in a cone. The liquid is indicated by shading. H is the height of the cone's apex above the bulk liquid surface, h is the height of the meniscus, h_c is the height of the contact line, r_c is the radius of the contact line, α is the half-angle of the cone opening, ψ is the contact angle of the liquid, Δh is the distance from the bottom of the meniscus to the tip, R_s is the radius of the spherical meniscus, and R_c is the distance from the contact line to the tip.

$$\frac{E}{\gamma_{lv}L_c^2} = \frac{A}{4} \left(\frac{\Delta h}{L_c}\right)^4 + \frac{B}{3} \left(\frac{H}{L_c}\right) \left(\frac{\Delta h}{L_c}\right)^3 + \frac{C}{2} \left(\frac{\Delta h}{L_c}\right)^2, \quad (1)$$

where we have expressed all lengths in terms of the capillary length, which is the characteristic length scale for problems in hydrostatics involving gravity and surface tension.¹³ The capillary length is given by $L_c = \sqrt{\gamma_{lv}/\rho g}$, where γ_{lv} is the liquid-vapor surface tension, ρ is the liquid density, and g is the acceleration of gravity. The characteristic energy scale is $\gamma_{lv}L_c^2$. Hereafter, we choose units such that $\gamma_{lv}L_c^2 = 1$ and $L_c = 1$.

In Appendix A, we show that the expansion in Eq. (1) is exact in the approximation that the meniscus is spherical and calculate the coefficients A , B , and C explicitly (they depend only on the half-angle of the cone α and the contact angle ψ .) For the physically relevant range of parameters, $A > 0$ and $B < 0$; $C > 0$ if $\psi < \pi/2$, but may have either sign, depending on the value of α if $\psi > \pi/2$. In Appendix B, we investigate the validity of the approximation that the meniscus is spherical.

Equation (1) can be generalized to the case where the pressure in the open space at the tip of the cone exceeds the pressure over the external bath by an amount ΔP (as in the classical problem of a cylindrical barometer). The work done by the gas on the meniscus when it moves can be taken into account by a term $-\Delta P V_{open}$ in the free energy, where V_{open} is the volume of the open space. Because $V_{open} \propto \Delta h^3$, this term has the same effect in Eq. (1) as offsetting H by a constant. We take $\Delta P = 0$ (equal pressure inside and outside the cone) in what follows.

We now turn to the solution of the problem posed by the minimization of the free energy in Eq. (1). The equilibrium positions of the meniscus are determined by the condition that the generalized force $F_{gen} = -\partial E/\partial \Delta h$ equals zero,

$$F_{gen} = -A\Delta h^3 - B H \Delta h^2 - C \Delta h = 0, \quad (2)$$

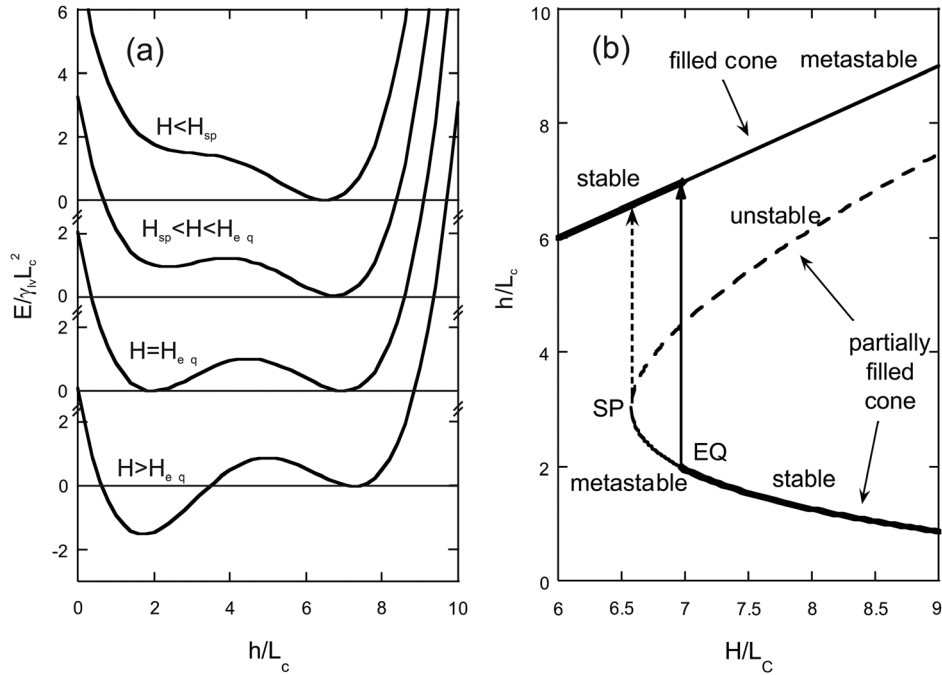


Fig. 4. (a) The energy as a function of the meniscus height h , expressed in units of the capillary length L_c , for various values of the cone height H . (The curves are offset vertically for clarity.) When the position of the cone is above the equilibrium point ($H > H_{eq}$), the energy has two local minima: the partially filled cone is stable and the filled cone is metastable. When the cone is at the equilibrium point ($H = H_{eq}$), the partially filled cone and the completely filled cone have equal energies. When the cone is between the equilibrium point and the spinodal ($H_{sp} < H < H_{eq}$), the filled cone is the stable state, and the partially filled cone is metastable. If the cone is lower than the spinodal ($H < H_{sp}$), the only stable state is the filled cone. (b) The equilibrium heights of a wetting meniscus (contact angle $\psi = 0$) in a cone of half-angle $\alpha = 12^\circ$. The heavy solid line shows the globally stable root of Eq. (2), the light solid line is locally stable, and the dashed branch is unstable. As the cone is lowered in the liquid, EQ indicates the point where the meniscus would jump to the top of the cone if the system were always in the state of lowest energy. In practice, the energy barrier is too high for the jump to occur at EQ, and the meniscus may not jump until the system reaches the spinodal at SP.

which has one or three real roots, depending on the discriminant $D = \sqrt{(BH)^2 - 4AC}$, as shown in Fig. 4. One root is $\Delta h = 0$, which corresponds to the cone being completely filled. The other two roots are

$$\Delta h_{\pm} = \frac{-BH \pm D}{2A}. \quad (3)$$

The condition for equilibrium to be stable is that the energy be a minimum, $\partial^2 E / \partial \Delta h^2 > 0$. For the root $\Delta h = 0$, $\partial^2 E / \partial \Delta h^2|_{\Delta h=0} = 2C$. For the other roots, we have

$$\left. \frac{\partial^2 E}{\partial \Delta h^2} \right|_{\Delta h_{\pm}} = \frac{D(D \mp BH)}{2A}. \quad (4)$$

We first consider $C > 0$, which is the case if the contact angle $\psi < \pi/2$ (see Fig. 4). If $C > 0$, the totally filled cone ($\Delta h = 0$) is always stable. Because $BH < 0$ and $0 < D < -BH$, we find that the root at Δh_+ is always stable, and Δh_- is unstable. The free energy in the state Δh_- is a maximum, not a minimum, and corresponds to the free energy barrier for the transition between the two stable states. This barrier vanishes when the state Δh_+ ceases to be a local minimum, which occurs when $D = 0$, which is thus a spinodal in this mean-field model. The height of the cone at the spinodal is given by

$$H_{sp} \equiv \sqrt{4AC/B^2}. \quad (5)$$

As the system approaches the spinodal, the free energy barrier vanishes as $\Delta E \sim \frac{4}{3}|B|^{3/2}C^{5/4}A^{-7/4}(H - H_{sp})^{3/2}$. At the spinodal, the height of the meniscus is given by

$$\Delta h_{sp} = \sqrt{C/A}. \quad (6)$$

Finally, we ask which root is globally stable, $\Delta h = 0$ or Δh_+ . The crossover point occurs when $E(0) = E(\Delta h_+)$, which occurs when the cone is at height $H_{eq} \equiv \sqrt{9AC/2B^2}$.

As we lower the cone slowly into the liquid, we trace out the heavy solid curve in Fig. 4 if the meniscus is always in equilibrium, with the meniscus jumping to the top of the cone at the point labeled EQ, which is the coexistence point. For a macroscopic system, the barrier for the jump is large compared to $k_B T$ ($\gamma_v L_c^2 / k_B T$ is on the order of 10^{10} for our system), and we should be able to come close to the spinodal H_{sp} before jumping to the filled cone at the point labeled SP (the dashed arrow in Fig. 4).

In principle, there is no spinodal for the reverse jump when the cone is drawn out of the liquid. The reverse jump will occur when the cone has been drawn high enough that the energy barrier for forming a gas bubble at the tip of the cone is small enough to be overcome by vibrations or other perturbations of the system. In our experiment the tip of the cone is cut off, and hence the cone is not quite in the stable minimum represented by $\Delta h = 0$ when it is filled, and the ‘‘filled’’ state may become unstable at some point as the cone is raised slowly out of the bath.

If $C < 0$, which may occur if $\psi > \pi/2$, then the totally filled cone ($\Delta h = 0$) is always an unstable state. The discriminant

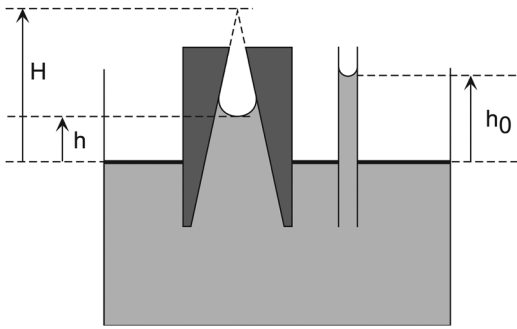


Fig. 5. Experimental apparatus. A cone is lowered into a liquid bath; the height of the meniscus in the cone (h) and the position of the bath level with respect to the cone (H) are determined from optical images, or from the capillary rise h_0 in a straight capillary.

D is always real and greater than BH , so that both Δh_{\pm} are real. However, $\Delta h_- < 0$, so this root is not physical. The state $\Delta h = \Delta h_+$ is stable and is the only allowed state. For such non-wetting surfaces, there is no attraction to draw the meniscus to the apex of the cone.

III. EXPERIMENT

The transition of the meniscus height is easily observed by dipping a transparent cone into a liquid, as illustrated in Fig. 5. (The cone may be dipped by hand, with care.) Alternatively, the cone may be fixed and the level of the liquid raised. The tip of the cone must be open to allow air to escape as the cone is dipped into the liquid bath. A plastic pipette cap with the tip cut off is suitable, or a cone may be cast in transparent polydimethylsiloxane (PDMS) on a machined metal cone in a rectangular external mold.

Suitable liquids include isopropanol, silicone oil (Rhodorsil V50), and tetradecane, which wet the cone materials (contact angle $\psi = 0$). The experiment would be difficult to perform with non-wetting liquids, because the meniscus would be pinned on any defects in the surface of the cone. The capillary length $L_c = 1.48, 1.64,$ and 1.88 mm for silicone oil,¹⁴ isopropanol,¹⁵ and tetradecane,¹⁵ respectively. If PDMS cones are used, they should be immersed in the liquid for at least 5 days before experiments are made, because PDMS is a highly porous material that absorbs a large amount of liquid. During swelling, large deformations occur, and the apparent contact angle is nonzero. If the polymerization is homogeneous, the shape of the cone is not modified,

although the increase in linear dimensions is of the order of 15%.

Some other precautions must be taken to ensure reproducibility of the experiment. The cone must be lowered (or the liquid level raised) slowly to ensure that the meniscus is in local equilibrium. If the rate of descent is too fast ($5 \mu\text{m/s}$ or more), viscous effects make the position of the meniscus lag behind the equilibrium position. Furthermore, for isopropanol/plastic and tetradecane/PDMS, we have observed that the meniscus sticks at certain points in some of our cones. For these materials it might be that the liquid does not wet the cone perfectly (the contact angle ψ is small but not exactly zero), so the meniscus can be temporarily pinned on defects in the cone's surface. As long as the jump does not take place near a sticking point, and the cone is lowered slowly enough, the position of the jump is reproducible for most of our cones to within $10 \mu\text{m}$ from run to run—a negligible error compared to the uncertainty of the position of the cone tip.

Some typical results are presented in Figs. 6–9. In these experiments, the cone is dipped slowly into the liquid bath using a computer controlled translation stage at rates from 0.2 to $10 \mu\text{m/s}$. The position of the meniscus is determined directly from video images. The height h of the meniscus must be measured with respect to the height of the liquid bath, which varies during the experiment due to the volume of the fluid displaced by the cone as it descends. The height of the free surface is measured by looking at the meniscus outside the cone or, as illustrated in Fig. 5, by observing the capillary rise h_0 in a straight cylindrical capillary of known radius r using Jurin's law,¹⁶ $h_0 = 2L_c^2/r$. The height of the apex of the cone H is initially determined by extrapolating the sides of the cone in the image. When the cone is in motion, the displacement of the apex is determined from the position of the translation stage. The extrapolation is the largest source of error in the experiment, especially when the half-angle α of the cone is small and the cone is cut far from the apex. For our experiments in a cone made from a plastic pipette cap, the extrapolated position of the apex may be off by a constant as large as 0.5 mm. For the PDMS cone the uncertainty is smaller by a factor of 2.

Figure 6 illustrates the effect of dipping a plastic cone ($\alpha = 5.5^\circ$) into isopropanol. For up to 53 s, the meniscus gradually rises as the cone descends. After 55 s, the meniscus starts to ascend rapidly toward the tip of the cone. Therefore, between these two frames the partially filled state has changed from metastable to unstable.

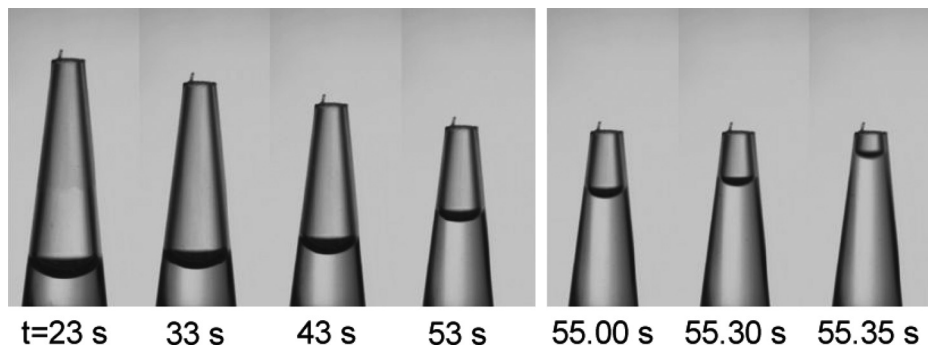


Fig. 6. A plastic pipette cap is slowly lowered into isopropanol. After 53 s, the meniscus starts to move toward the tip of the cone. Vertical scale: 7.1 mm

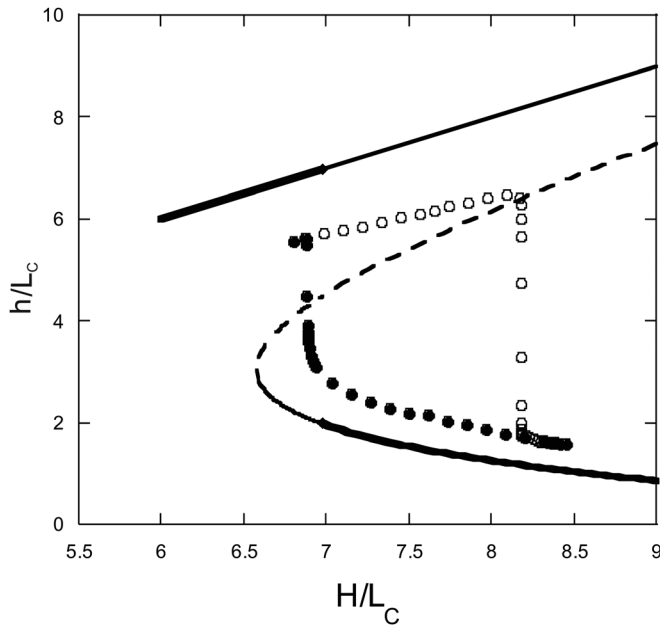


Fig. 7. The meniscus height as a function of cone position as measured for silicone oil in a PDMS cone of half-angle $\alpha = 12^\circ$ (every third point is shown for clarity). Filled circles: cone descending (decreasing H); open circles: cone ascending (increasing H). The height of the meniscus in the “filled cone” state is not equal to the height of the cone, because the tip of the cone is truncated.

Figure 7 illustrates the experimental results for silicone oil in a PDMS cone with $\alpha = 12^\circ$. Because the main uncertainty is locating the position of the tip of the cone and the reference level of the liquid, we show in Fig. 8 the data for the cone descending with an offset determined by fitting the data to the prediction of Eq. (6) (the offsets are $0.32L_c$ in H and $0.44L_c$ in h). Plotting the data on logarithmic axes shows that the system comes within $\approx 2.5 \times 10^{-3} L_c$ of H_{sp} before jumping.

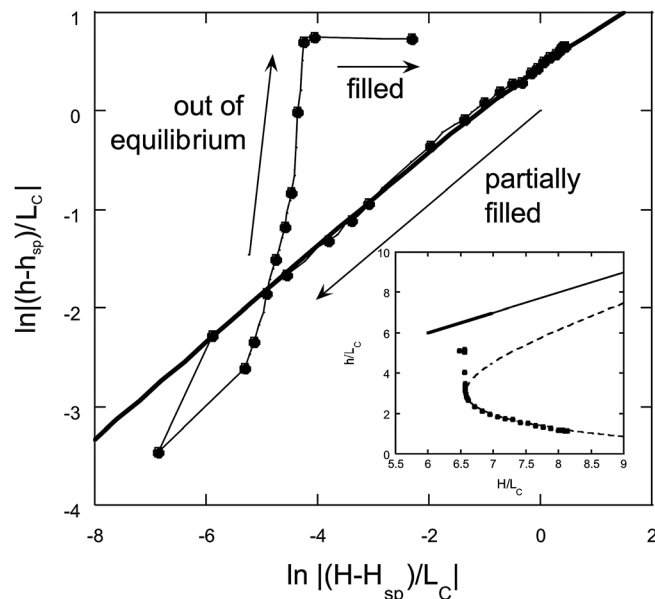


Fig. 8. The meniscus height as a function of the cone position as measured for silicone oil in a descending PDMS cone of half-angle $\alpha = 12^\circ$. The circles show the same data as in Fig. 7, offset by a constant to match the calculation (inset). The main graph shows that the meniscus approaches within $2.5 \times 10^{-3} L_c$ of the spinodal before jumping, and that the critical behavior at the spinodal matches the calculation.

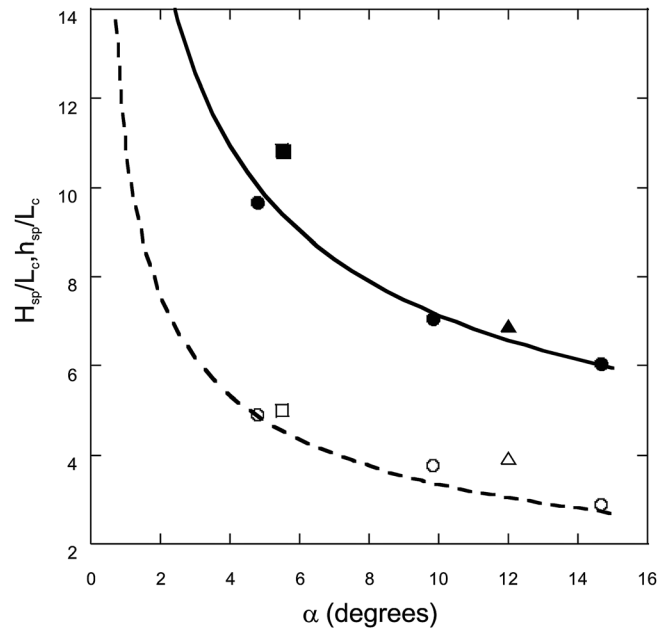


Fig. 9. Measurements of the height of the cone at the spinodal, H_{sp} (solid symbols), compared to the prediction of Eq. (5) (solid curve), and measurements of the height of the meniscus at the spinodal, h_{sp} (open symbols), compared with the prediction of Eq. (6) (dashed curve), as a function of the half-angle of the cone, α . Circles: tetradecane/PDMS; squares: isopropanol/plastic; triangles: silicone oil/PDMS. The error bars are comparable to the size of the symbols.

The results for several values of α and combinations of liquid and substrate are summarized in Fig. 9. The agreement between theory and experiment is good, with the exception of the data for isopropanol on the plastic pipette tip, where the liquid may not be perfectly wetting.

IV. SUMMARY

Spinodal decomposition plays a role in many applications of technological importance. We have presented a macroscopically observable experiment on wetting in a conical geometry, illustrating a first-order phase transition and a spinodal point. Both experiment and theory for the wetting system are accessible to undergraduates.¹⁷

A variety of avenues for further exploration of this interesting system are available for advanced students. By imposing vertical oscillations on the system, the susceptibility $\partial h/\partial H$ as a function of frequency can be measured. The resonant frequency of the system vanishes at the spinodal, and the DC susceptibility diverges. A white noise source would model the effects of temperature.

ACKNOWLEDGMENTS

The authors wish to thank the Ecole Normale Supérieure and the Université de Paris Diderot for support, Alexis Prévost for help with casting the PDMS, and Milton Cole, Silvina Gatica, and Sébastien Balibar for fruitful discussions.

APPENDIX A: THE ENERGY OF A PARTIALLY FILLED CONE

The energy difference between a partially filled cone and a completely filled cone can be calculated as follows. Let H be the height of the cone, α its half-angle, ψ the

contact angle of the liquid, and h the height of the meniscus, as shown in Fig. 3. It is convenient to determine the energy in terms of the distance of the meniscus from the apex, $\Delta h = H - h$. We start with the assumption that the meniscus is spherical (we will show in Appendix B that this assumption is very good) and has radius R_S . In that case, it is useful to note that the open volume above the meniscus scales in proportion to Δh^3 , but does not change shape when the meniscus moves.

The cost of creating the free surface of the liquid and baring part of the cone wall is

$$E_{\text{surface}} = \gamma_{lv}A_l + (\gamma_{wv} - \gamma_{lw})A_w, \quad (\text{A1})$$

where γ_{lv} , γ_{lw} , and γ_{wv} are the liquid-vapor, liquid-wall, and wall-vapor surface tensions, respectively, and A_l and A_w are the surface areas of the meniscus and of the bare part of the cone wall. The Young-Dupré law¹⁰ yields $(\gamma_{wv} - \gamma_{lw}) = \gamma_{lv}\cos\psi$. The surface areas are given by $A_l = 2\pi R_S^2[1 + \sin(\alpha - \psi)]$, where $A_w = \pi R_C^2 \sin\alpha$, and R_C is the distance from the tip of the cone to the contact line, as illustrated in Fig. 3. The geometry of Fig. 3 gives $R_C = R_S \cos(\alpha - \psi) / \sin\alpha$ and $R_S = \Delta h / (1 + \cos\psi / \sin\alpha)$. Note that E_{surface} is proportional to Δh^2 .

The gain in gravitational potential energy due to lowering the meniscus from the top of the cone to height h is given by

$$E_{\text{grav}} = - \int_{V_{\text{open}}} \rho g z dV = -\rho g \int_h^H \pi r^2 z dz, \quad (\text{A2})$$

where ρ is the density of the liquid (minus the density of the gas, if the latter is non-negligible), V_{open} is the open volume above the meniscus, and $r(z)$ is the radius of the open volume at height z . From the geometry, $r^2 = R_S^2 - (R_S + h - z)^2$ for $h < z < h_C$ and $r = (H - z)\tan\alpha$ for $h_C < z < H$, where h_C is the height of the contact line, given by $h_C = h + R_S[1 + \sin(\alpha - \psi)]$. If we change the variable of integration in Eq. (A2) to $z' = H - z$, where z' measures the height downward from the tip of the cone, then

$$\begin{aligned} E_{\text{grav}} &= - \int_{V_{\text{open}}} \rho g (H - z') dV \\ &= \rho g \int_0^{\Delta h} \pi r^2 z' dz' - \rho g H \int_0^{\Delta h} \pi r^2 dz'. \end{aligned} \quad (\text{A3})$$

The first term on the right-hand side of Eq. (A3) is proportional to Δh^4 and the second to $H\Delta h^3$.

If we add Eqs. (A1) and (A3), we find that the energy difference between the partially filled cone and the completely filled cone is given by

$$\frac{E}{\gamma_{lv}L_c^2} = \frac{A}{4} \left(\frac{\Delta h}{L_c}\right)^4 + \frac{B}{3} \left(\frac{H}{L_c}\right) \left(\frac{\Delta h}{L_c}\right)^3 + \frac{C}{2} \left(\frac{\Delta h}{L_c}\right)^2, \quad (\text{A4})$$

where $L_c = \sqrt{\gamma_{lv}/\rho g}$, and the coefficients A , B , and C are given by

$$\begin{aligned} A &= \frac{\pi \sin^2 \alpha}{6[1 + \sin(\alpha + \psi)]^2} \{7 + 2 \cos(2\alpha) - \cos[2(\alpha - \psi)] \\ &\quad - 2 \cos(2\psi) - 4 \sin(\alpha - \psi) + 8 \sin(\alpha + \psi)\}, \end{aligned} \quad (\text{A5})$$

$$\begin{aligned} B &= \frac{\pi \sin^2 \alpha}{2[1 + \sin(\alpha + \psi)]^2} [\cos(2\psi) + \sin(\alpha - \psi) \\ &\quad - 3 \sin(\alpha + \psi) - 3], \end{aligned} \quad (\text{A6})$$

and

$$C = \frac{2\pi[2 + 2 \sin(\alpha - \psi) + \cos^2(\alpha - \psi) \cos\psi / \sin\alpha]}{(1 + \cos\psi / \sin\alpha)^2}. \quad (\text{A7})$$

In the wetting case (contact angle $\psi = 0$), Eqs. (A5)–(A7) simplify (the derivation is simplified if we make this assumption from the start),

$$A = \frac{\pi \sin^2 \alpha (3 - \sin\alpha)}{3(1 + \sin\alpha)}, \quad (\text{A8})$$

$$B = -\frac{\pi \sin^2 \alpha}{1 + \sin\alpha}, \quad (\text{A9})$$

and

$$C = 2\pi \sin\alpha. \quad (\text{A10})$$

From the form of Eq. (A3), it is clear that for the physically relevant range of parameters, $0 < \alpha < \pi/2$, $0 < \psi < \pi$, $A > 0$, and $B < 0$, the coefficient $C > 0$ in the wetting case ($\psi = 0$). Numerical investigation of Eq. (A7) shows that $C > 0$ for all contact angles $0 < \psi < \pi/2$. For contact angles $\psi > \pi/2$, C can have either sign (note that $\partial C / \partial \alpha|_{\alpha=0} = 2\pi \cos\psi$).

APPENDIX B: THE EXACT SHAPE OF THE MENISCUS

Here, we discuss the assumption made in Appendix A that the meniscus is spherical in shape, which is valid if the meniscus is not too large compared to L_c . However, near the spinodal, the size of the meniscus is comparable to L_c , and the approximation must be checked. The exact shape, illustrated in Fig. 10(a), is governed by the Laplace equation, which for a surface of revolution can be written as

$$2 \times \text{mean curvature} = d\phi/ds + \sin\phi/r = z/L_c^2, \quad (\text{B1})$$

where r and z are the coordinates of the surface in cylindrical coordinates (z measured from the bulk liquid surface), ϕ is the angle between the local surface normal and the vertical direction, and s is the arc length along the meniscus. Equation (B1) can be integrated numerically using the parametric equations: $dr/ds = \cos\phi$, $dz/ds = \sin\phi$, and $d\phi/ds = -\sin\phi/r + z/L_c^2$. The integration starts at the bottom of the meniscus, with z equal to some arbitrary h and $r = 0$, and the initial conditions given by the requirement that the two curvatures start out equal at the bottom of the meniscus for a surface of revolution: $d\phi/ds = \sin\phi/r = h/2$ (thus ϕ also has an initial value of 0). The integration ends when the meniscus is tangent to the cone, that is, when $\phi = \alpha + \pi/2$ (see Fig. 3). The terminal point of the integration is the position of the contact line (h_C , r_C) shown in Fig. 3. The height of the apex H is determined by extrapolating the tangent line back to $r = 0$, that is, $H = h_C + r_C/\tan\alpha$, as illustrated in Fig. 10(a). The value of the cone height H determined by this procedure from the starting meniscus height h is plotted in Fig. 10(b). The result is double-valued, corresponding to the stable and unstable roots h_{\pm} . (The integration of the Laplace

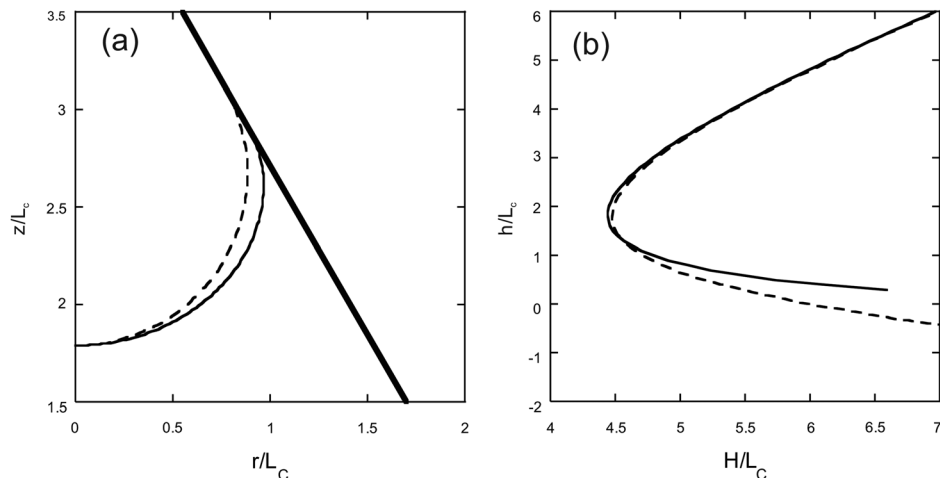


Fig. 10. The effect of approximating the shape of the meniscus by a sphere for a cone of half-angle $\alpha = 30^\circ$ and contact angle $\psi = 0$. (a) The light solid line shows the shape of the meniscus (height as a function of radius on a 1:1 scale) calculated from Laplace's equation, taking capillary forces and gravity into account exactly (light solid curve); the dashed line shows the spherical approximation. The side of the cone is drawn as a heavy solid line. (b) A plot of the equilibrium meniscus height as a function of cone position shows that near the spinodal, the spherical meniscus approximation (dashed curve, representing the meniscus positions h_{\pm}) is close to the results of the numerical integration of the Laplace equation (solid curve).

equation does not yield any results for non-equilibrium positions of the meniscus, because the shape of the meniscus it describes is an extremum of the free energy, and can be derived from a variational principle.¹⁸ It is nevertheless unusual that Laplace's equation can be used to find unstable equilibrium positions of the meniscus, as approximated by the root h_{\pm} . It can be seen that the spherical approximation accurately predicts the capillary rise near the spinodal, but it is less valid far from the spinodal (for instance, the spherical approximation implausibly predicts $h < 0$ for $H \gg H_{sp}$).

^aElectronic mail: mpettersen@washjeff.edu

¹L. D. Landau and E. M. Lifshitz, *Statistical Physics, Part 1*, 3rd ed. (Pergamon, Oxford, 1988), Sec. 162, Problem 2.

²H. Maris and S. Balibar, "Negative pressures and cavitation in liquid helium," *Phys. Today* **53**(2), 29–34 (2000).

³L. Gunther, "A comprehensive treatment of classical nucleation in a supercooled or superheated fluid," *Am. J. Phys.* **71**, 351–357 (2003).

⁴P. M. Chaikin and T. C. Lubensky, *Principles of Condensed Matter Physics* (Cambridge University, Cambridge, 1995), Sec. 8.7.

⁵K. Binder, "Nucleation barriers, spinodals, and the Ginzburg criterion," *Phys. Rev. A* **29**, 341–349 (1984); For a recent review, see K. Binder, "Spinodal decomposition versus nucleation and growth," in *Kinetics of Phase Transitions*, edited by S. Puri and V. Wadhawan (CRC, Boca Raton, 2009).

⁶J. W. Cahn, "Phase separation by spinodal decomposition in isotropic systems," *J. Chem. Phys.* **42**, 93–99 (1965).

⁷P.-G. de Gennes, "Dynamics of fluctuations and spinodal decomposition in polymer blends," *J. Chem. Phys.* **72**, 4756–4763 (1980).

⁸J. Erlebacher and R. Seshadri, "Hard materials with tunable porosity," *MRS Bull.* **34**, 561–568 (2009).

⁹J. Pellicer, José A. Manzanares, and Salvador Mafé, "The physical description of elementary surface phenomena: Thermodynamics versus mechanics," *Am. J. Phys.* **63**, 542–547 (1995).

¹⁰P.-G. de Gennes, F. Brochard-Wyart, and D. Quéré, *Capillarity and Wetting Phenomena: Drops, Bubbles, Pearls, Waves* (Springer, New York, 2004), Sec. 1.2.1.

¹¹Y. Tsoi, "Discontinuous meniscus location in tapered capillaries driven by pressure difference and dielectrophoretic forces," *Langmuir* **23**, 8028–8034 (2007).

¹²See for instance, E. H. Hauge, "Macroscopic theory of wetting in a wedge," *Phys. Rev. A* **46**, 4994–4998 (1992); K. Rejmer, S. Dietrich, and M. Napiórkowski "Filling transition for a wedge," *Phys. Rev. E* **60**, 4027–4042 (1999); S. M. Gatica, M. M. Calbi, and M. W. Cole, "Simple model of capillary condensation in porous media," *ibid* **65**, 061605-1–4 (2002).

¹³Reference 10, Sec. 2.1.

¹⁴For silicone oil Rhodorsil V50 $\gamma = 20.7$ mN/m and specific mass $\rho = 0.959$ g/cm³, www.bluestarsilicones.com/webdav/site/BSI/users/wendy/public/DOCUMENTS%20TELECHARGEABLES/HUILES%2047/Oils47_EN_V2010.pdf.

¹⁵For Tetradecane, $\gamma = 26.13$ mN/m and $\rho = 0.752$ g/cm³; for isopropanol $\gamma = 20.93$ mN/m and $\rho = 0.786$ g/cm³. J. J. Jasper, "The surface tension of pure liquid compounds," *J. Phys. Chem. Ref. Data* **1**, 841–1010 (1972).

¹⁶Reference 10, Sec. 2.4.

¹⁷For example, a student at Washington and Jefferson College did a summer project on building a setup similar to the one illustrated in this paper, and wrote a LABVIEW program to extract the meniscus height from the digital camera images.

¹⁸See, for instance, M. J. Smith, "Variational derivation of Young's law and Laplace's capillary equation," *Am. J. Phys.* **38**, 1153–1155 (1970).